This is the peer reviewd version of the followng article:

Ex vivo fluorescence confocal microscopy for intraoperative, real-time diagnosis of cutaneous inflammatory diseases: A preliminary study / Bertoni, L; Azzoni, P; Reggiani, C; Pisciotta, A; Carnevale, G; Chester, J; Kaleci, S; Reggiani Bonetti, L; Cesinaro, Am; Longo, C; Pellacani, G.. - In: EXPERIMENTAL DERMATOLOGY. - ISSN 0906-6705. - 27:10(2018), pp. 1152-1159. [10.1111/exd.13754]

Terms of use:

The terms and conditions for the reuse of this version of the manuscript are specified in the publishing policy. For all terms of use and more information see the publisher's website.

07/02/2025 06:25

(Article begins on next page)

DR. LAURA BERTONI (Orcid ID : 0000-0002-8994-8791)

Article type : Regular Article

Ex-vivo fluorescence confocal microscopy for intraoperative, real time diagnoses of cutaneous inflammatory diseases: a preliminary study

Running title: *FCM for diagnosis of inflammatory diseases*

Laura Bertoni[1*], Paola Azzoni[1], Camilla Reggiani[2], Alessandra Pisciotta[1], Gianluca Carnevale[1], Johanna Chester[2], Shaniko Kaleci[2], Luca Reggiani Bonetti[3], Anna Maria Cesinaro[4], Caterina Longo[5], Giovanni Pellacani[1,2]

[1]Department of Surgery, Medicine, Dentistry and Morphological Sciences with interest in Transplant, Oncology and Regenerative Medicine, University of Modena and Reggio Emilia, Modena, Italy;
[2]Department of Dermatology, University of Modena and Reggio Emilia, Italy;
[3]Department of Diagnostic, Clinic and Public Health Medicine, University of Modena and Reggio Emilia, Modena, Italy;
[4]Anatomic Pathology, Azienda Ospedaliero-Universitaria Policlinico, Modena, Italy;
[5]Arcispedale Santa Maria Nuova IRCCS, Arcispedale Santa Maria Nuova IRCCS, Reggio Emilia, Italy.

[*]**Corresponding author:**
Dr. Laura Bertoni
e-mail: laura.bertoni@unimore.it

This article has been accepted for publication and undergone full peer review but has not been through the copyediting, typesetting, pagination and proofreading process, which may lead to differences between this version and the Version of Record. Please cite this article as doi: 10.1111/exd.13754
This article is protected by copyright. All rights reserved.

Accepted Article

ABSTRACT

Ex vivo Fluorescence Confocal Microscopy (FCM) is an innovative imaging tool that can be used intraoperatively to obtain real-time images of untreated excised tissue with almost histologic resolution. Since inflammatory diseases often share overlapping clinical features, histopathology evaluation is required for dubious cases, delaying definitive diagnoses, and therefore therapy.

This study identifies key-features at *ex vivo* FCM for differential diagnoses of cutaneous inflammatory diseases, in particular psoriasis, eczema, lichen planus and discoid lupus erythematosus. Retrospective *ex vivo* FCM and histological evaluations with relevant diagnoses were correlated with prospectively reported histopathologic diagnoses, to evaluate agreement and the level of expertise required for correct diagnoses.

We demonstrated that *ex-vivo* FCM enabled the distinction of the main inflammatory features in most cases, providing a substantial concordance to histopathologic diagnoses. Moreover, *ex vivo* FCM and histological evaluations reached a substantial agreement with histopathologic diagnoses both for all raters, and for each operator. After a yet to be defined learning curve, these preliminary results suggest that dermatologists may be able to satisfactorily interpret *ex vivo* FCM images for correct real time diagnoses.

Despite some limitations mainly related to the equipment of FCM with a single objective lens, our study suggests that ex vivo FCM seems a promising tool in assisting diagnoses of cutaneous inflammatory lesions, with a level of accuracy quite close to that offered by histopathology. This is the first study to investigate *ex vivo* FCM application in cutaneous inflammatory lesions, and to evaluate the diagnostic capability of this technology.

Key words: *Ex-vivo* FCM, psoriasis, eczema, lichen planus, discoid lupus erythematosus.

This article is protected by copyright. All rights reserved.

Accepted Article

Accepted Article

INTRODUCTION

Ex-vivo fluorescence confocal microscopy (FCM) is an emerging diagnostic tool, which enables real time images with nuclear level resolution of fresh tissue excisions. Vertical section images of the whole tissue biopsy, labelled with fluorescent dye, can be obtained, whilst the integrity of the biopsy is maintained. These images are comparable to frozen section and routine histopathology and can be analysed directly in the operating room [1]. As the *ex-vivo* FCM imaging process does not alter the examined tissue, the same specimen can be used for histopathological and immunohistochemical examinations.

Ex-vivo FCM has been successfully applied to surgical skin specimens to analyse a wide range of neoplastic and non-neoplastic lesions, as well as to define surgical margins during intraoperative evaluation [1-10], but with a few studies showing its value in other solid organ cancers [11, 12]. However, *ex-vivo* FCM has never been applied to cutaneous inflammatory diseases, one of the most common motives for dermatological visits and biopsies. Inflammatory diseases often present in many forms, from occasional rashes accompanied by skin itching and redness, to chronic conditions such as psoriasis, eczema, lichen planus and discoid lupus erythematosus (LED). Within each of these pathologies there are some similar clinical and histopathological appearances and etiologies, which have been widely studied and characterized [13-19].

Since inflammatory diseases share multiple and overlapping clinical features, differential diagnoses for the dermatologist can be complicated [20, 21]. Therefore, in dubious cases, evaluation at histopathology for certain diagnoses is the current gold standard. However, time is required between biopsy and diagnosis, prior to which treatment cannot be initiated. *Ex-vivo* FCM may provide real time indications for differential diagnosis, enabling anticipated diagnosis.

This article is protected by copyright. All rights reserved.

The aim of the current study was to verify the capability to identify histopathologic key-features for the diagnosis of inflammatory skin diseases on pseudo-histopathologic images generated by FCM. Features and diagnoses were correlated with histopathology to estimate agreement. As a second objective, the level of expertise required for correct diagnoses was assessed.

METHODS

Study population

From June 2016 to May 2017, 147 cutaneous lesions, obtained from the Dermatology Unit of Modena (Italy), were examined with *ex-vivo* FCM (VivaScope® 2500 *ex-vivo*; Mavig, Munich, Germany). For the current study, inflammatory lesions referred to biopsy for diagnosis were selected. Further exclusion criteria included lesions with aspecific diagnoses at histology, < 2 identified lesions per inflammatory disease type and lesions with low quality *ex-vivo* FCM images. A total of 20 lesions LED. The study was approved by the Ethics Committee for Policlinico of Modena (protocol number 4267/2015) and written informed consent was obtained from each patient within the European project "Diagnoptics" (CIP-PSP programme, number 621066).

Specimen evaluations

Common histopathological features for inflammatory diseases [14, 17] were hypothetically selected according to potential visibility at routine haematoxylin and eosin (H&E)-stained histopathology for each inflammatory disease type by an expert dermatologist with experience in dermatopathology (G.P.) and a board-certified dermatopathologist (A.M.C.). These parameters were defined and are outlined in Table 1.

All selected *ex-vivo* FCM images and histological slides were stored in a dedicated database. The images were randomly displayed to each of the three professionals: 1 dermatopathologist (AMC), 1 general pathologist (LR) and 1 dermatologist with experience in confocal

This article is protected by copyright. All rights reserved.

Accepted Article

microscopy and dermatopathology (CR). All professionals were blinded to histopathologic diagnoses, and were asked to retrospectively identify the presence or absence of defined parameters first on *ex-vivo* FCM images. Diagnoses for the 20 *ex-vivo* FCM images were made (*ex-vivo* FCM diagnoses).

The same experts were subsequently presented with randomly displayed histological slides of the same 20 lesions and asked to identify the presence or absence of the same defined parameters for an eventual diagnosis (histological evaluation). All examinations were performed independently. Lesions were grouped according to official prospective diagnoses at histopathology (histopathological diagnoses).

Specimens and staining procedure

Specimens were freshly excised from inflammatory lesions. Lesion biopsies, taken with a 6-8 mm biopsy punch (Kai Medical, Japan), were vertically sectioned in order to correlate results with histopathological diagnoses; the biopsies were divided, and half was stained for *ex-vivo* FCM imaging and the other half was placed in formalin in a biopsy container (Biopsafe, Thermalyne®). During the staining process the tissue samples were completely immersed for 30 seconds in 10% citric acid (Sigma-Aldrich®), washed in physiological saline solution, then soaked for 30 seconds in acridine orange solution (0.6 mM; Sigma-Aldrich®) and washed again in physiological saline solution. The sample was placed on absorbent paper prior to being compressed between two glass slides, in order to obtain tissue flatting and avoid border flipping, and sealed with silicon glue. They were then positioned onto the stage of the FCM.

Instrument

The *ex-vivo* FCM Vivascope 2500® (Lucid Inc; Rochester NY, USA) has 3 lasers, which enables tissue examination in reflectance (830 nm) and/or fluorescence (488 nm and 658 nm) modalities. In our study, both reflectance (830nm) and fluorescence (488 nm only) modes were acquired consecutively for each tissue examination. For *ex-vivo* FCM diagnoses images

Accepted Article

This article is protected by copyright. All rights reserved.

acquired in the fluorescence mode were utilized only. Other technical parameters of the *ex-vivo* FCM include a maximum examination depth of 200 μm, a vertical resolution of up to 4 μm, a magnification of 550×, a maximum scan size of 32 × 24 mm (single field of view 550 μm × 550 μm, and a mosaic style reconstruction of the tissue composed of 2860 images (square shaped images of 1024 × 1024 pixels). The laser filter has a 38×, 0.85 numerical aperture water immersion objective lens. The software VivaScan® (Version 11, Mavig GmbH, Munich, Germany) enables the reconstruction of the images from the probes, with the VivaBlock® tool (acquisition of multiple images in the X/Y directions within a single plane at a fixed depth) and the VivaStack® tool (permits a survey of multiple frames along the Z axis, visualizing deeper tissue). In this study, the staining and imaging processes were completed within 10 minutes. Following the acquisition of *ex-vivo* FCM images, stained samples were also formalin fixed and both stained and unstained samples were sent for histopathological examination

Statistical analysis

The Cohen's kappa (κ) statistic has been used to measure the agreement between histopathology features identified at *ex-vivo* FCM and histopathology. Moreover, κ was also calculated in the evaluation of the agreement between the final operator diagnosis and histopathological diagnosis. We evaluated inter-observer agreement for both histological and *ex-vivo* FCM diagnoses. We selected κ statistic as the measure of agreement because our variable of interest is binary [22].

Kappa is a measure of the level of agreement, indicating a less than chance ($\kappa < 0$), slight (κ = 0.01 to 0.20), fair (κ = 0.21 to 0.40), moderate (κ = 0.41 to 0.60), substantial (κ = 0.61 to 0.80), almost perfect (κ = 0.81 to 0.99) and perfect ($\kappa = 1$) agreement. P indicates the level of agreement between the two methodologies. A $P<0.05$ was considered significant.

This article is protected by copyright. All rights reserved.

Accepted Article

RESULTS

Psoriasis

Standard features associated with correct psoriasis diagnoses at histology include psoriasiform hyperplasia, parakeratosis, dilated capillaries, perivascular and interstitial inflammatory infiltrate, subcorneal/intracorneal pustules and hypogranulosis (Fig. 1A-E). As shown in Figure 1F, *ex-vivo* FCM mosaics presented a psoriasiform hyperplasia characterized by thin, elongated rete ridges of nearly equal lengths of keratinocytes with highly fluorescent nucleus. When *ex-vivo* FCM images were digitally zoomed, the presence of parakeratosis, consisting in hyper-reflective nuclei in the superficial stratum corneum (Fig 1G) was appreciable. Furthermore, dilated capillaries were recognized in papillary dermis near the lower limit of the epidermis as dark tortuous vessels surrounded by flat nuclei (Fig. 1H). As a further diagnostic clue, in the upper dermis a dense amount of hyper-reflective small round nuclei was observed among dermal fibers and surrounding the vessels, which corresponds to a perivascular and interstitial infiltrate of lymphocytes, as revealed by H&E staining (Fig. 1I). Interestingly, the presence of bilobate or trilobated hyper-reflective nuclei in the upper layers of the epidermis (spinous layer and/or stratum corneum) was detected, resembling neutrophils nuclei (Munro's microabscesses). In particular, such nuclei were surrounded by black empty spaces, which might correspond to sub-corneal or intra-corneal pustules (Fig. 1L). Other important evidence for the diagnosis of psoriasis is hypogranulosis, which was only indirectly detectable by accurately focusing on the upper part of the epidermis; cells resembled the basal epithelial layer due to an incomplete shape modification of epithelial cells towards a flattening appearance, typical of corneal epidermal scales.

The agreement between the identification of these features at *ex-vivo* FCM and histological evaluation was almost perfect for the inflammatory infiltrate (κ =0.84), substantial for psoriasiform hyperplasia, parakeratosis and dilated vessels (κ = 0.72, 0.67 and 0.61

This article is protected by copyright. All rights reserved.

respectively) and only fair for subcorneal pustules (κ = 0.36), as shown in Table 1. The percentage of correct diagnoses of psoriasis for all raters in FCM evaluation and histological evaluation with respect to histopathological diagnoses were both 90.5% (Table S1). The diagnosis of psoriasis had the highest reliability of all the 4 types of lesions.

Eczema

At histology, H&E staining shows eczema specific features: irregular hyperplasia, hyper-orthokeratosis, spread inflammatory infiltrate and spongiosis (Fig. 2A-D). As reported in Figure 2E, the *ex-vivo* FCM image enables the identification of the presence of hyperplasia, corresponding to a thick layer of hyper reflecting keratinocytes, characterized by irregular ridges, due to inflammatory injury followed by epidermal proliferation. In digitally zoomed images, hyper-orthokeratosis, recognizable as a nuclei-free, thick corneal stratum laying on the epidermis surface, was clearly detectable (Fig. 2F). A further feature shown in Figure 2G included superficial perivascular mild inflammatory infiltrate, which resulted to be characterized by the presence of bright small round and well defined nuclei. Another diagnostic signature might be given by the presence of spongiosis, characterized by the presence of intraepidermal and intercellular edema at histology, whereas at *ex-vivo* FCM images evidenced widened intercellular black spaces among adjacent keratinocytes (Fig. 2H). The concordance existing between *ex-vivo* FCM eczema features and corresponding histological evaluation was detected in Table 1. The agreement for irregular hyperplasia and hyper-ortokeratosis was moderate (κ = 0.48 and 0.52 respectively), for inflammatory infiltrate was almost perfect (κ = 0.84) while for spongiosis is less than chance (κ = -0.08). The percentage of correct diagnoses for eczema in *ex-vivo* FCM and histological evaluation vs histopathological diagnoses were 66.7% and 76.2% respectively for all raters (Table S1), and was the least reliable diagnosis of the 4 types of lesions included in the current study.

This article is protected by copyright. All rights reserved.

Accepted Article

Lichen planus

From a histological point of view, lichen planus images show a dense band-like cellular infiltrate spread throughout the superficial dermis, irregular epidermal hyperplasia with a sawtooth appearance, compact orthokeratosis and a hypergranulosis (Fig. 3A-D)

Ex-vivo FCM images showed a dense superficial infiltrate immediately underlying the epidermal surface and parallel to it, identifiable as a diffuse compact band of highly fluorescent small spots, spread throughout the superficial dermis (Fig. 3E). In Figure 3F the digitally zoomed images revealed the presence of irregular jagged epidermal hyperplasia with sawtooth appearance in which hyper reflective keratinocytes are arranged in a layer with a denticular profile. The stratum corneum appeared thickened and compacted without nuclei, a typical feature of compact orthokeratosis (Fig. 3G). Moreover, hypergranulosis, which implies an increased thickness of the stratum granulosum with cells containing granules, was recognized as groups of cells with hypofluorescent big nuclei surrounded by small granules, hardly recognizable in *ex-vivo* FCM images (Fig. 3H).

Table 1 showed the agreement of these features between *ex-vivo* FCM and histological evaluation. In particular the concordance was moderate for compact orthokeratosis ($\kappa = 0.52$), substantial for sawtooth epidermal hyperplasia ($\kappa = 0.62$), almost perfect for lichenoid infiltrate ($\kappa = 0.89$) and slight for hypergranulosis ($\kappa = 0.05$). For all raters the percentage of correct diagnoses between *ex-vivo* FCM and histological evaluation of lichen planus compared to histopathologic diagnoses were both 83% (Table S1), with a high diagnostic reliability.

This article is protected by copyright. All rights reserved.

Accepted Article

Accepted Article

LED

Histological evaluation of LED is mostly characterized by deep periadnexal and perivascular inflammatory infiltrate that has the tendency to accumulate around the pilosebaceous follicles and sebaceous glands (Fig. 4A-B). Other features are thinned epidermis (Fig. 4C), orthokeratosis and basal cell vacuolization (Fig. 4D).

As reported in Figures 4E and F, *ex-vivo* FCM images showed the presence of a deep inflammatory infiltrate, with hyperfluorescent small dense dots with a characteristic periadnexal and perivascular localization. Thinned epidermis and orthokeratosis were evident in Figure 4G as a slim band of highly fluorescent keratinocytes with a thick corneal stratum standing above. Furthermore, interface reaction, taking shape by a dark vacuolar change throughout the Dermo-Epidermis Junction (DEJ), is well appreciable (Fig. 4H).

A clear agreement between *ex-vivo* FCM features and the corresponding histological evaluation was shown in Table 1. The concordance was less than chance for orthokeratosis ($\kappa = -0.02$), moderate for discontinued DEJ/vacuolization ($\kappa = 0.47$) and substantial for perivascular inflammatory infiltrate ($\kappa = 0.68$) and thin epidermis ($\kappa = 0.63$). The percentage of correct diagnoses for LE in *ex-vivo* FCM and histological evaluation vs histopathologic diagnoses reached 83% and 100% respectively (Table S1), suggesting a high reliability at *ex-vivo* FCM and a perfect diagnosis at histological evaluation.

For each of the 3 participating operators, the agreement between diagnoses at *ex-vivo* FCM and histology was estimated, based on official histopathological diagnoses (the current gold standard). Diagnoses were perfectly matched between the acridine orange stained and unstained portions of biopsies. The dermatopathologist obtained a perfect agreement at histopathology evaluation ($\kappa = 1$) and a substantial agreement at *ex-vivo* FCM images ($\kappa =$

This article is protected by copyright. All rights reserved.

Accepted Article

0.79). The experienced dermatologist and general pathologist both obtained a substantial agreement at histological and *ex-vivo* FCM analyses (κ =0.71 and κ =0.72, and κ =0.64 and κ =0.65, respectively).

DISCUSSION

Ex-vivo FCM is an emerging diagnostic tool that allows intraoperative real-time analysis of tissue specimens. Images of thick sections of freshly excised tissue can be acquired after fluorescent dye labelling. In the current study, acridine orange was selected because it has been proven to only stain DNA, providing a strong contrast between nuclear morphology and the surrounding background [23-24], without altering tissue morphology [1]. To date, *ex-vivo* FCM has been evaluated for its correlation with the histopathology in healthy skin [24], its application in diagnosis of basal cell carcinoma [4, 7, 9, 25, 26, 27], squamous cell carcinoma [28, 29], rare malignant adnexal tumours, such as the eccrine syringomatous carcinoma [30], and conjunctival lesion evaluation in ophthalmology [31], for assessment of tumour margins on fresh tissue excisions in Mohs surgery. Other application was the differential diagnosis of melanocytic lesions from healthy skin [10, 32, 33]. Interestingly, *ex-vivo* FCM was found effective in prompt evaluations of solid organ tumors, extending its possible application to the general surgical oncology [11,12].

The aim of this study was to analyse *ex-vivo* FCM images of cutaneous inflammatory lesions and to evaluate/measure their correlation with the corresponding histopathological specimens. Among inflammatory diseases, our study focused on psoriasis, eczema, lichen planus and LED.

We demonstrated that the application of *ex-vivo* FCM enabled differential diagnosis of 4 of the main inflammatory diseases in most cases, providing a substantial agreement to histopathological diagnoses for all four inflammatory diseases investigated.

This article is protected by copyright. All rights reserved.

In *ex-vivo* FCM images of psoriasis, the most easily identifiable, but not disease specific feature, was the presence of inflammatory infiltrate. Psoriasiform hyperplasia, parakeratosis, and dilated vessels were well distinguishable, while subcorneal pustules were the most difficult feature to recognize.

When diagnosing eczema, again the non-disease specific feature of inflammatory infiltrate was well assessable, while irregular hyperplasia and hyper-orthokeratosis were moderately in agreement with histological evaluation. Spongiosis revealed to be very difficult to identify in *ex-vivo* FCM.

In lichen planus lesions, the most easily recognizable specific feature was lichenoid infiltrate, and decreasingly identifiable were sawtooth epidermal hyperplasia and compact orthokeratosis. For lichen planus, hypergranulosis was revealed to be difficult to identify at *ex-vivo* FCM.

In LED, perivascular inflammatory infiltrate and thin epidermis were easily recognizable at *ex-vivo* FCM, whereas discontinued DEJ showed only a moderate agreement. Orthokeratosis resulted to be unidentifiable in *ex-vivo* FCM.

According to Hartmann et al., *ex-vivo* FCM has some technical limitations. Sectioning of the tissue is performed manually, and can be irregular, depending upon the skill of the operator. Further, the horizontal pressure applied on the slide may be uneven, with some parts of the sample not adhering to the object slide and thus resulting in poor quality scanned images with blurred or missing parts [33]. In this study, 33% of inflammatory lesions with specific ≥2 histopathology diagnoses/lesion type were excluded due to poor image quality. In the current study, some features associated, such as spongiosis, subcorneal pustoles and hypergranulosis were difficult to visualise and obtained a lower agreement than more general morphological features with histological image identification. This could derive to the use of fresh tissue, and some features, such as spongiosis and subcorneal pustoles, enhanced by histopathology

This article is protected by copyright. All rights reserved.

Accepted Article

process artifacts, may result less easily visible. Further, the presence of a single objective lens limited detailed images to digital zooming only. The use of higher magnification objectives could improve image resolution, enabling better visualization of details of cell morphology.

Despite these limits, the percentages of correct diagnoses reported in *ex-vivo* FCM evaluation were encouraging when compared to the gold standard histopathology evaluation, both for all raters and for the individual operators. Given these considerations, our study suggests that *ex-vivo* FCM seems a promising tool in assisting in cutaneous inflammatory lesions diagnoses, with a level of accuracy quite close to that offered by histopathology.

The secondary aim of the study was to estimate the level of expertise required for correct diagnoses at *ex-vivo* FCM. According to the double-blinded study design, the diagnoses at *ex-vivo* FCM and histological evaluation by the 3 operators with different levels of experience were evaluated. As expected, a dedicated board certified dermatopathologist was found to be more likely to find a higher agreement in *ex-vivo* FCM analyses, compared to a dermatologist and a general histopathologist. However, the capabilities of the dermatologist and of the general histopathologist were the same for *ex-vivo* FCM and histological evaluations compared to histopathological diagnoses. An overall substantial agreement was established between all the raters for all diagnoses.

These observations suggest that correct diagnoses with *ex-vivo* FCM may be achievable by dermatology professionals following a learning curve, which is yet to be defined. Moreover, the installation of image sharing technologies could provide real-time, intra-operative consultation with an experienced specialist or dermatopathologist for dubious diagnoses, especially useful during the learning curve. Histopathological diagnosis represents the diagnostic gold standard to ascertain the nature of clinically dubious inflammatory lesions. Nevertheless, histopathology requires time-consuming procedures to process samples and

Accepted Article

This article is protected by copyright. All rights reserved.

diagnosis is delayed. The quick feasibility of *ex-vivo* FCM examination may enable a more timely patient therapy management.

However, this study is primarily limited by the small sample size and outcomes should be interpreted with caution. The current study cannot support the introduction of this technology into daily practice, as it is too small to prove sensitivity, specificity, and predictive values. Larger studies are required to confirm the *ex-vivo* FCM features for evaluation of each inflammatory lesion type for correlation with histopathology. Furthermore, the technical addition to *ex-vivo* FCM of higher magnification objectives and a more efficient procedure for tissue flattening should improve image quality and resolution and the ability to identify morphological details, such as subcellular structures, thereby further enhancing the potential diagnostic reliability of *ex-vivo* FCM and its correlation with histopathology.

In this preliminary study, *ex-vivo* FCM seems to be a promising tool in offering real-time differential diagnoses of cutaneous inflammatory diseases, but correct interpretation of *ex-vivo* FCM images seems to require a high level of specific expertise, comparable to histopathology. Further studies are needed to evaluate the learning curve required for correct *ex-vivo* FCM image interpretation.

Authors' contribution: LB, PA designed and performed most of the experiments, collected and analyzed data, and drafted the manuscript; CR, AMC, LRB performed histological and FCM evaluations and drafted the manuscript; AP, GC collected data, assisted with image analysis and drafted the manuscript; JC, SK performed statistical analysis, interpreted data and assisted with manuscript draft; CL supervised the experimental design and assisted with data interpretation; GP obtained funding, supervised the experimental design. All authors reviewed and approved the manuscript.

This article is protected by copyright. All rights reserved.

Accepted Article

Accepted Article

Acknowledgments: This study was supported by the Diagnoptics CIP-PSP programme European Grant (Diagnoptics CIP-PSP programme, number 621066).

Conflicts of Interest: None declared.

REFERENCES

[1] Gareau DS, Li Y, Huang B et al. Confocal mosaicing microscopy in Mohs skin excisions: feasibility of rapid surgical pathology. J Biomed Opt 2008;13:054001.

[2] Gareau DS, Patel YG, Li Y et al. Confocal mosaicing microscopy in skin excisions: a demonstration of rapid surgical pathology. J Microsc 2009;233:149–59.

[3] Kaeb S, Landthaler M, Hohenleutner U. Confocal laser scanning microscopy – evaluation of native tissue sections in micrographic surgery. Lasers Med Sci 2009;24:819–23.

[4] Karen JK, Gareau DS, Dusza SW, et al. Detection of basal cell carcinomas in Mohs excisions with fluorescence confocal mosaicing microscopy. Br J Dermatol 2009;160:1242–1250.

[5] Bennàssar A, Vilalta A, Carrera C et al. Rapid diagnosis of two facial papules using *ex-vivo* fluorescence confocal microscopy: toward a rapid bedside pathology. Dermatol Surg 2012;38:1548–51.

[6] Abeytunge S, Li Y, Larson B, et al. Confocal microscopy with strip mosaicing for rapid imaging over large areas of excised tissue. J Biomed Opt 2013;18:61227.

[7] Longo C, Rajadhyaksha M, Ragazzi M, et al. Evaluating ex-vivo fluorescence confocal microscopy images of basal cell carcinomas in Mohs excised tissue. Br J Dermatol 2014;171:561- 570.

This article is protected by copyright. All rights reserved.

Accepted Article

[8] Białek-Galas K, Wielowieyska-Szybińska D, Dyduch G, et al. The use of reflectance confocal microscopy in selected inflammatory skin diseases. Pol J Pathol 2015;66(2):103-108.

[9] Longo C, Ragazzi M, Rajadhyaksha M, et al. In Vivo and Ex-vivo Confocal Microscopy for Dermatologic and Mohs Surgeons. Dermatol Clin 2016;34:497–504.

[10] Hartmann D, Krammer S, Vural S, et al. Immunofluorescence and confocal microscopy for ex-vivo diagnosis of melanocytic and non-melanocytic skin tumors: A pilot study. J Bio-photonics 2018;11(3).

[11] Schiffhauer LM, Boger JN, Bonfiglio TA, et al. Confocal microscopy of unfixed breast needle core biopsies: a comparison to fixed and stained sections. BMC Cancer 2009;9:265.

[12] Ragazzi M, Piana S, Longo C, et al. Fluorescence confocal microscopy for pathologists. Mod Pathol 2014;27(3):460-71.

[13] Pinkus H, Mehregan AH. The primary histologic lesion of seborrheic dermatitis and psoriasis. J Invest Dermatol 1966;46:109–116.

[14] Ackerman, AB. Histologic Diagnosis of Inflammatory Skin Diseases: A Method by Pattern Analysis.Philadelphia: Lea & Febiger; 1978.

[15] Barr RJ, Young EM Jr. Psoriasiform and related papulosquamous disorders. J Cutan Pathol 1985;12:412-425.

[16] Sweet WL, Smoller BR. Differential proliferation of endothelial cells and keratinocytes in psoriasis and spongiotic dermatitis. J Cutan Pathol 1997;24:356–363.

[17] Weedon D. Weedon's Skin Pathology. China: Churchill Livingstone; 2010.

[18] Joshi R. Interface dermatitis. Indian J Dermatol Venereol Leprol 2013;79(3):349-59.

[19] Gru AA. Introduction to inflammatory dermatoses: Histological clues for the practicing pathologist. Semin Diagn Pathol 2017;34(3):210.

This article is protected by copyright. All rights reserved.

Accepted Article

[20] Aydin O, Engin B, Oguz O, et al. Non-pustular palmoplantar psoriasis: is histologic differentiation from eczematous dermatitis possible? J Cutan Pathol 2008;35:169–173.

[21] Goldsmith L, Katz S, Gilchrest B, et al. Fitzpatrick's Dermatology in General Medicine, 8th edition. New York: Mc Graw Hill, 2012.

[22] Cohen J. A coefficient of agreement for nominal scales. Educational and Psychological Measurement 1960;20(1):37-46.

[23] Inoue H, Kudo SE, Shiokawa A. Technology insight: Laser-scanning confocal microscopy and endocytoscopy for cellular observation of the gastrointestinal tract. Nat Clin Pract Gastroenterol Hepatol 2005;2:31-37.

[24] Hartmann D, Ruini C, Mathemeier L, et al. Identification of ex-vivo confocal scanning microscopic features and their histological correlates in human skin. et al. J Biophotonics. 2016;9(4):376-87.

[25] Bennàssar A, Carrera C, Puig S, et al. Fast evaluation of 69 basal cell carcinomas with *ex-vivo* fluorescence confocal microscopy: criteria description, histopathological correlation, and interobserver agreement. JAMA Dermatol 2013;149:839–847.

[26] Espinasse M, Cinotti E, Grivet D, et al. 'En face' *ex-vivo* reflectance confocal microscopy to help the surgery of basal cell carcinoma of the eyelid. Clin Exp Ophthalmol 2017;45:442-447.

[27] Hartmann D Krammer S, Bachmann MR et al. Simple 3-criteria-based ex vivo confocal diagnosis of basal cell carcinoma. J Biophotonics. 2018 May 3:e201800062. doi: 10.1002/jbio.201800062.

[28] Longo C, Ragazzi M, Gardini S, et al. Ex-vivo fluorescence confocal microscopy in conjunction with Mohs micrographic surgery for cutaneous squamous cell carcinoma. J Am Acad Dermatol 2015; 73:321–322.

This article is protected by copyright. All rights reserved.

Accepted Article

[29] Ex vivo confocal microscopy features of cutaneous squamous cell carcinoma. Hartmann D, Krammer S, Bachmann MRet al. J Biophotonics. 2018 Apr;11(4):e201700318. doi: 10.1002/jbio.201700318.

[30] Longo C, Ragazzi M, Gardini S, et al. Ex-vivo Fluorescence Confocal Microscopy of Eccrine Syringomatous Carcinoma: A Report of 2 Cases. JAMA Dermatol 2015;151:1034–1036.

[31] Iovieno A, Longo C, de Luca M, et al. Fluorescence Confocal Microscopy for Ex-vivo Diagnosis of Conjunctival Tumors: A Pilot Study. Am J Ophthalmol 2016; 68:207–216.

[32] Hartmann D, Krammer S, Ruini C, et al. Correlation of histological and ex-vivo confocal tumor thickness in malignant melanoma. Lasers Med Sci 2016;31:921–927.

[33] Hartmann D, Ruini C, Mathemeier L, et al. Identification of ex-vivo confocal laser scanning microscopic features of melanocytic lesions and their histological correlates. J Biophotonics 2017;10: 128–142.

This article is protected by copyright. All rights reserved.

Table 1. ***Ex-vivo*** **FCM features of inflammatory lesions**

Lesion frequencies, κ and significance compared to histopathological evaluations for all raters are illustrated. The features are typical of psoriasis[1], eczema[2], lichen planus[3] and LED[4]. *$P<0.05$, ***$P<0.001$.

All raters		Histological evaluation			
***Ex-vivo* FCM evaluation**		No	Yes	κ - value	Level of agreement
Parakeratosis [1]	No	27	7	0.67***	Substantial
	Yes	3	23		
Hyper-orthokeratosis [2]	No	33	7	0.52***	Moderate
	Yes	6	14		
Compact orthokeratosis [3]	No	33	7	0.52***	Moderate
	Yes	6	14		
Orthokeratosis [4]	No	57	1	-0.02	Less than chance
	Yes	2	0		
Psoriasiform hyperplasia [1]	No	33	2	0.72***	Substantial
	Yes	6	19		
Irregular hyperplasia [2]	No	36	9	0.48***	Moderate
	Yes	4	11		
Sawtooth epidermal hyperplasia [3]	No	50	4	0.62***	Substantial
	Yes	1	9		
Thin epidermis [4]	No	52	2	0.63***	Substantial
	Yes	2	4		
Subcorneal pustules [1]	No	44	5	0.36*	Fair
	Yes	6	5		
Spongiosis [2]	No	48	9	-0.08	Less than chance
	Yes	3	0		
Hypergranulosis [3]	No	43	15	0.05	Slight
	Yes	1	1		
Discontinued DEJ/vacuolization [4]	No	49	5	0.47***	Moderate
	Yes	2	4		
Dilated vessels [1]	No	40	6	0.61***	Substantial
	Yes	3	11		
Inflammatory infiltrate [1 2]	No	15	3	0.84***	Almost perfect
	Yes	1	41		
Lichenoid infiltrate [3]	No	48	0	0.89***	Almost perfect
	Yes	2	10		
Perivascular inflammatory infiltrate [4]	No	57	2	0.68***	Substantial
	Yes	2	5		

This article is protected by copyright. All rights reserved.

Accepted Article

Accepted Article

FIGURE LEGENDS

Figure 1.

Psoriasis. Histological images (A-E) and *ex-vivo* FCM correlates acquired in fluorescence mode (488 nm) (F-L). Initial images (A, F) show psoriasiform hyperplasia. Zoomed images reveal parakeratosis (B, G), dilated vessels (C, H), inflammatory infiltrate (D, I), the presence of cells suggestive of neutrophils within the subcorneal pustules (E, L), as indicated by arrowheads. Scale bar = 50 µm.

Figure 2.

Eczema. Histological (A-D) and *ex-vivo* FCM corresponding images acquired in fluorescence mode (488 nm) (E-H). Initial images evidence irregular hyperplasia (A, E). Zoomed images show hyper-orthokeratosis (B, F), inflammatory infiltrate (C, G) and spongiosis (D, H). These features are indicated by the arrowheads. Scale bar = 50 µm.

Figure 3.

Lichen planus. Histological images (A-D) and *ex-vivo* FCM correlates acquired in fluorescence mode (488 nm) (E-H). Initial images show lichenoid infiltrate (A, E). Features highlight with zooming include the sawtooth epidermal hyperplasia (B e F), compact orthokeratosis (C, G), hypergranulosis (D, H) as indicated by arrowheads. Scale bar = 50 µm.

Figure 4.

LED. Histological images (A-D) and *ex-vivo* FCM correlates acquired in fluorescence mode (488 nm) (E-H). Initial images reveal inflammatory infiltrate with periadnexal and perivascular distribution (A, E). Zoomed images show deep inflammatory infiltrate around

This article is protected by copyright. All rights reserved.

the pilosebaceous follicles and sebaceous glands (yellow arrowheads) (B, F), thinned epidermis (yellow arrowheads) (C, G), orthokeratosis (red arrowheads) and basal cell vacuolization (yellow arrowheads) (D, H). Scale bar = 50 μm.

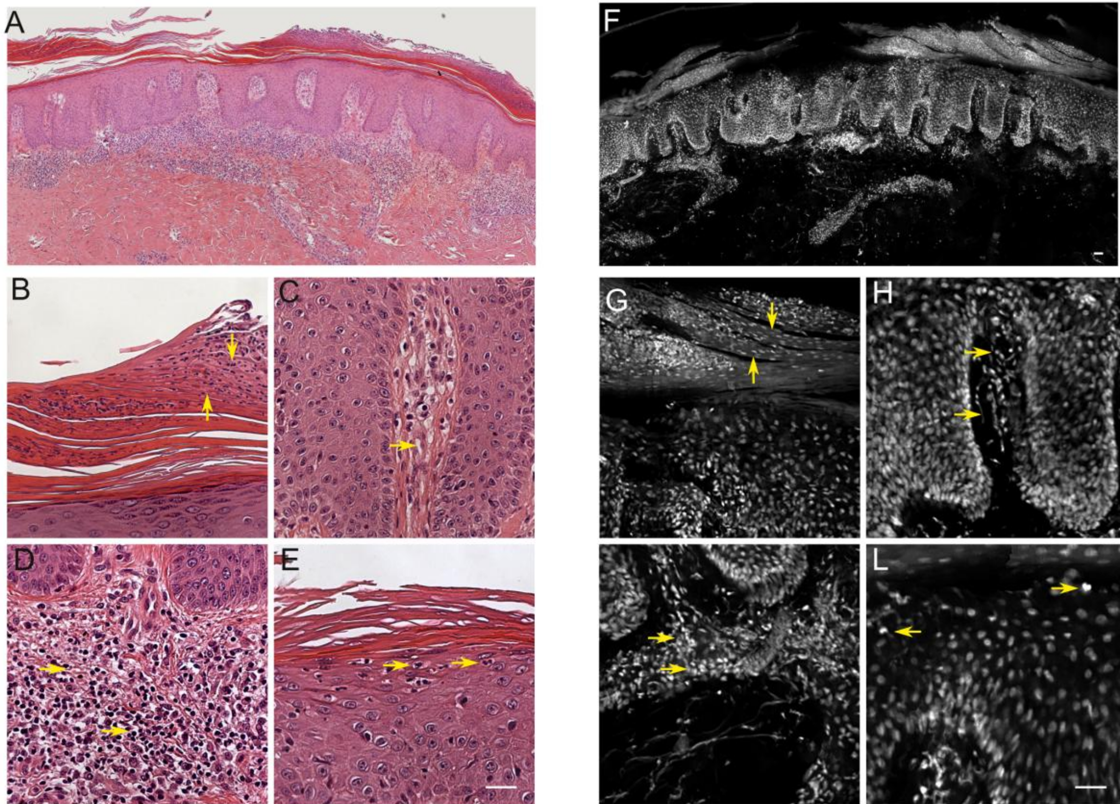

Accepted Article

This article is protected by copyright. All rights reserved.

Accepted Article

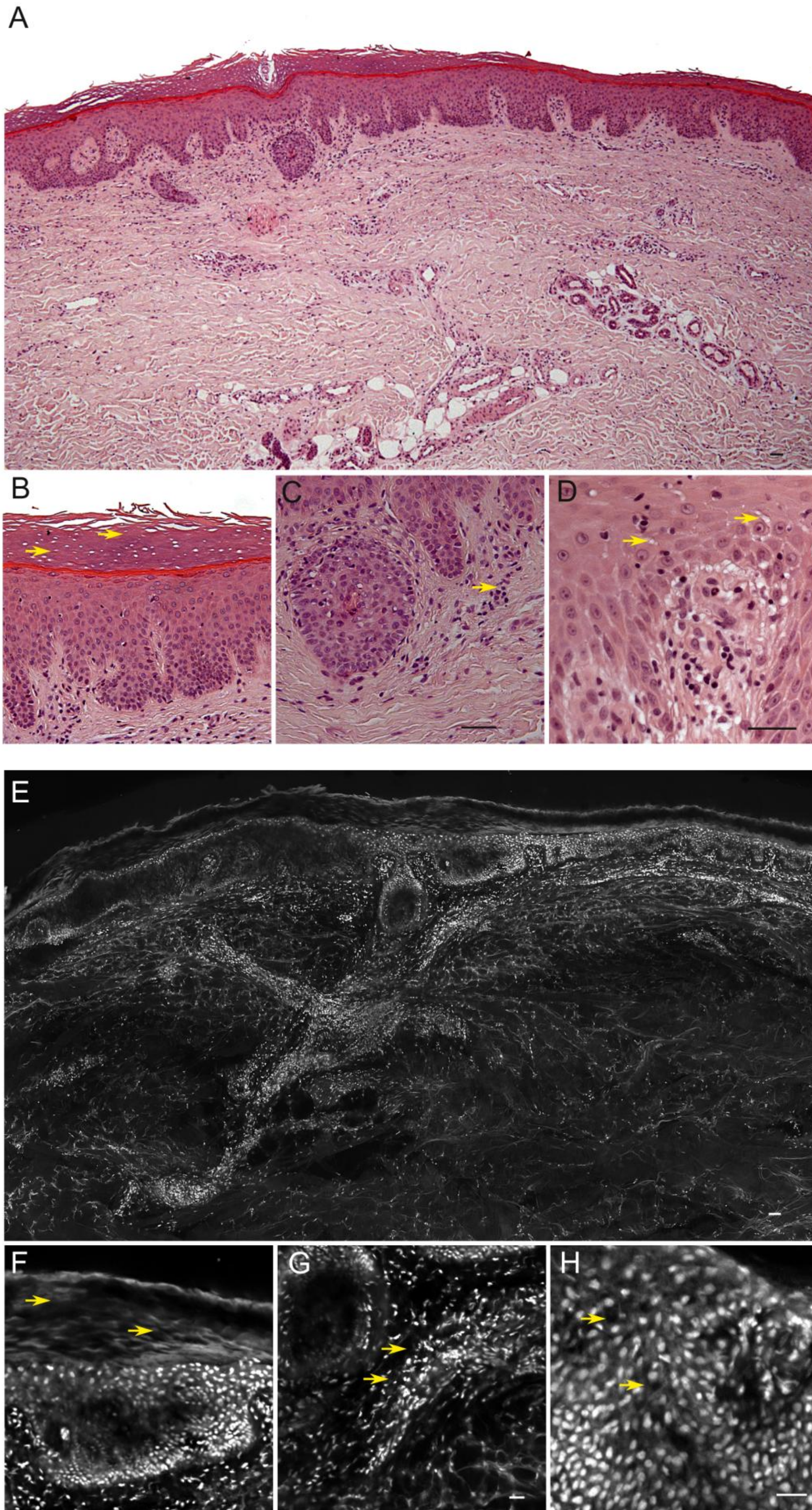

This article is protected by copyright. All rights reserved.

Accepted Article

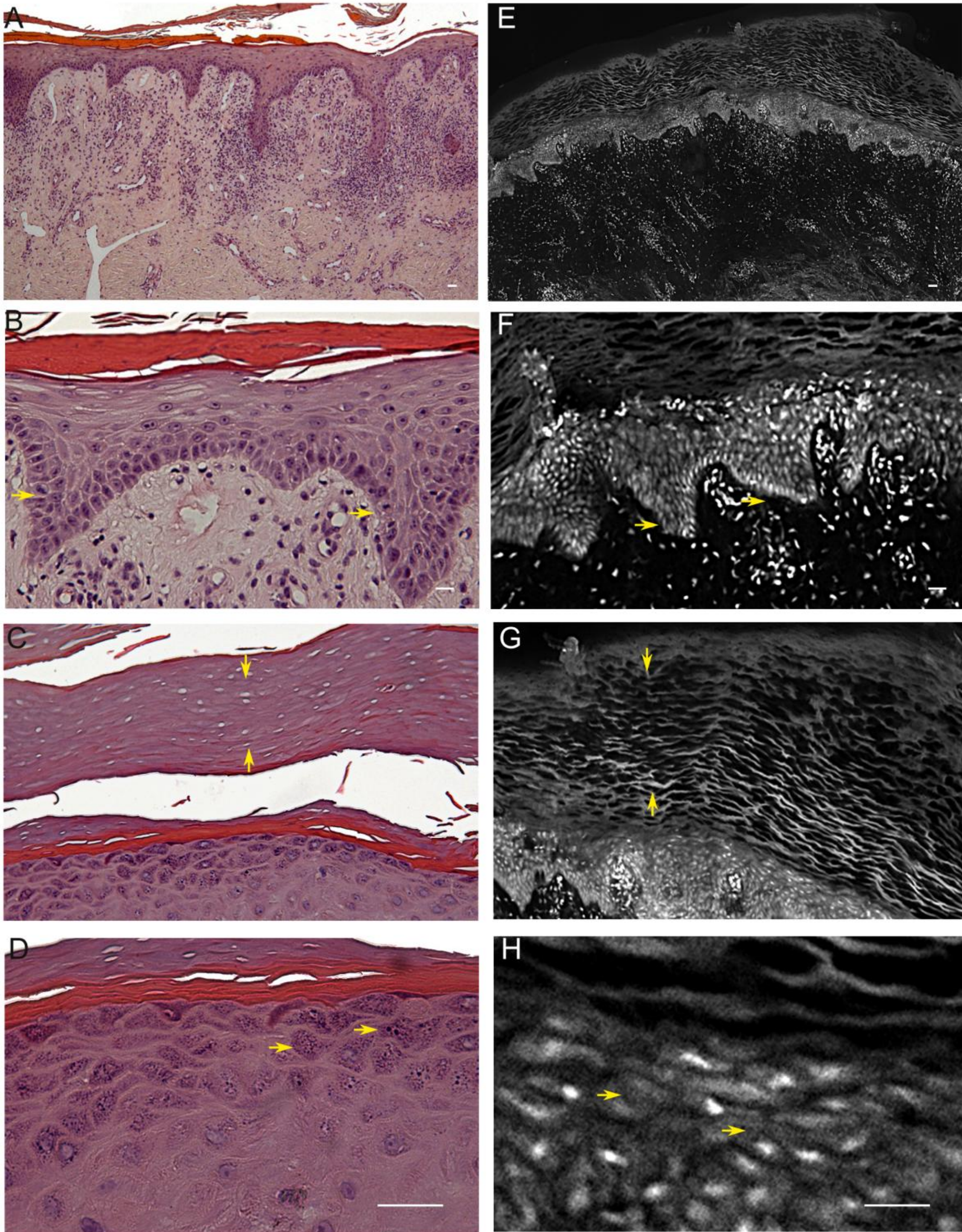

This article is protected by copyright. All rights reserved.

Accepted Article

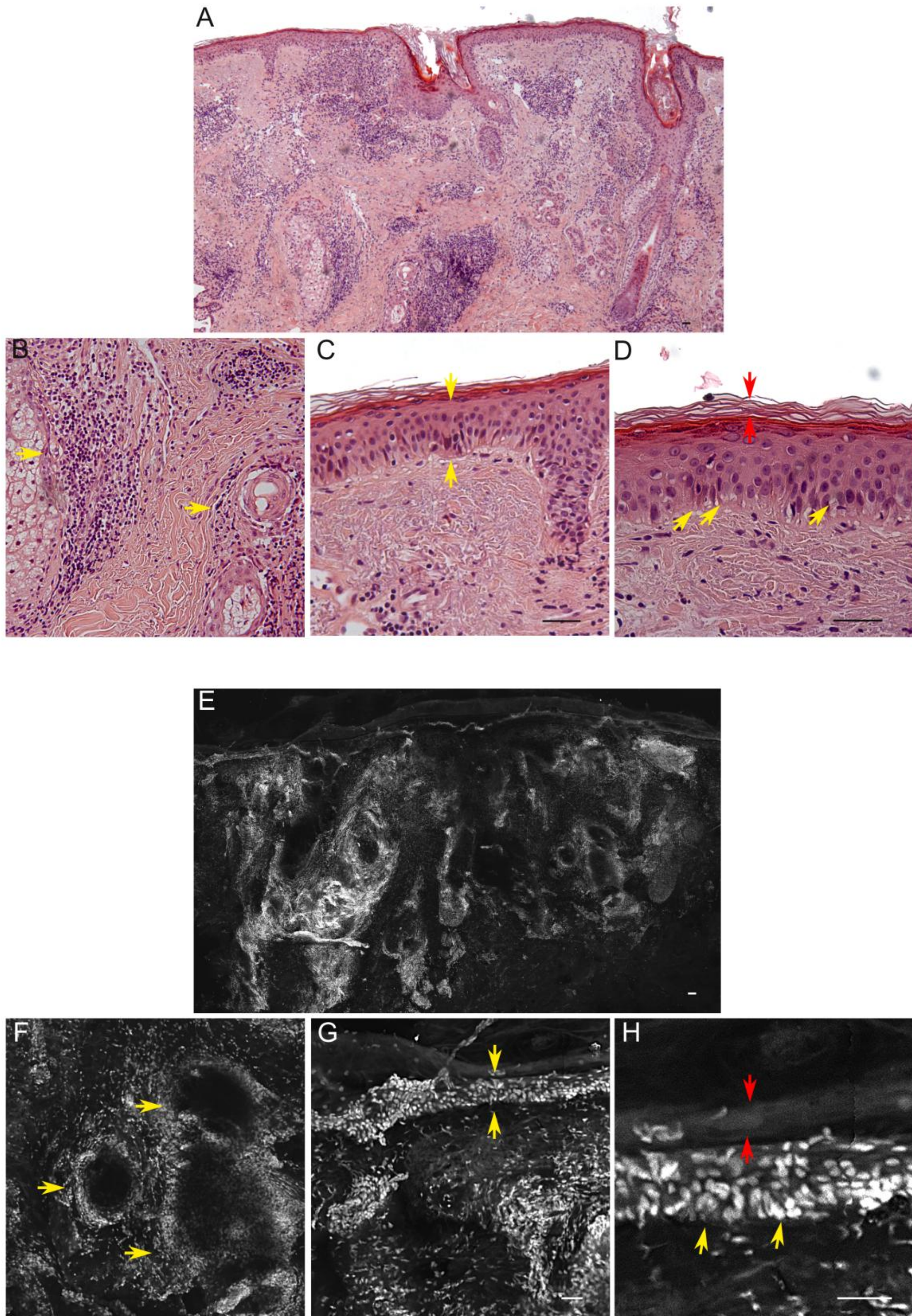

This article is protected by copyright. All rights reserved.